 CMES, vol.78, no.3, pp.185-208, 2011

Inverse Analysis of Solidification Problems Using the Mesh-Free Radial Point Interpolation Method

A. Khosravifard[1] **and M.R. Hematiyan**[1,2]

Abstract: An inverse method for optimal control of the freezing front motion in the solidification of pure materials is presented. The inverse technique utilizes the idea of a pseudo heat source to account for the latent heat effects. The numerical formulation of this inverse method is based on a formerly introduced meshless technique. In this method, the flux and the velocity of the liquid-solid interface are treated as secondary variables and the liquid and solid domains are modeled simultaneously. Some numerical examples are provided to demonstrate the efficiency of the presented method. The effects of regularization and the number of nodes of the proposed meshless method are investigated in the examples.

Keywords: Inverse analysis, Solidification, Meshless methods, pseudo heat source.

1 Introduction

In a direct solidification problem, boundary conditions on the boundaries of the problem domain are specified, and the objective is to find the time-dependent location of the moving solid-liquid interface. However, in an inverse solidification problem, the boundary conditions, at least on some parts of the boundary are usually unknown. The inverse solidification problems are often considered as design problems, in that, the objective is to find the unknown boundary conditions in order to obtain a specific pattern of solidification front. It is well known that controlling the morphology of the solid-liquid interface during the solidification process is of utmost importance to the formation of microstructure in the solidified materials [Okamoto and Li (2007)]. In case of solidification of a molten metal, controlling

[1] Department of Mechanical Engineering, Shiraz University, Shiraz, Iran.

[2] Corresponding author. Address: Department of Mechanical Engineering, Shiraz University, Shiraz, Iran. Tel.: +98 711 6133149; fax: +98 711 6473511. E-mail addresses: khosravifard@shirazu.ac.ir (A. Khosravifard), mo.hematiyan@gmail.com, mhemat@shirazu.ac.ir (M.R. Hematiyan)

the speed and pattern of the solidification front can have a great impact on the mechanical, as well as metallurgical properties of the solidified metal. By controlling the velocities at the freezing front, one can optimize the solidification time for different parts in a mold for a desired characteristic.

Numerical methods are usually used for the inverse analysis of practical solidification problems. In these methods, two conventional strategies can be utilized, i.e. the fixed grid techniques, and the moving or deforming grid techniques. The former incorporates the enthalpy formulation to account for the latent heat effects, while the latter continuously tracks the moving boundary by considering deforming grids or elements. There is also a third technique for the inverse analysis of solidification problems, which has found less attention in the literature. In this technique, the latent heat effect is accounted for, by considering a pseudo heat source near the freezing front. The idea of using a pseudo heat source for consideration of the latent heat effects can reduce or eliminate the nonlinearity of the inverse solidification problem. By this approach, the inverse analysis of a solidification problem reduces to a simple inverse heat conduction problem, involving a heat generation source [Hematiyan and Karani (2003)]. Although this method is not as accurate as the other two techniques, it can yield acceptable results with a much less computational labor.

Historically, the finite and boundary element methods have been the most important numerical tools for the analysis of the inverse solidification problems. Katz and Rubinsky (1984) were among the first ones who used the finite element method (FEM) for the inverse analysis of solidification processes in one-dimensional problems. Zabaras et al. utilized the boundary element method (BEM) for the design of casting processes. Their method was aimed at finding a specific boundary flux history that would result in a desired solidification front motion that is required to control the liquid feeding to the front [Zabaras, Mukherjee, and Richmond (1998)]. Zabaras (1990) also provided an FEM methodology for the solution of several one-dimensional solidification problems. Ruan and Zabaras (1991) utilized the FEM for determination of the interface location in 2D melting problems. Their method focused on the analysis and design of welding processes. Voller (1992) presented an enthalpy-based inverse algorithm for the inverse analysis of two-phase Stefan problems. Later, Zabaras et al. presented a methodology for finding the boundary flux or temperature for obtaining a desired motion of the freezing interface in two-dimensional problems [zabars, Ruan, and Richmond (1992)]. Zabaras and Yuan (1994) presented a dynamic programming methodology for the inverse analysis of Stefan problems. Their method was aimed at finding a heat flux history on the boundary so as to achieve a pre-defined movement of the solid-liquid interface. Kang and Zabaras (1995) proposed an adjoint method for calculation of the opti-

mum boundary cooling history in two-dimensional conduction driven solidification processes, for obtaining a desired history of the freezing interface motion. The inverse analysis of solidification problems in the presence of natural convection has also been performed. Zabaras and Nguyen (1995) presented a methodology for control of freezing front morphology in solidification problems. In their analysis they considered the effect of natural convection in the liquid region. Frankel and Keyhani (1996) used a weighted residual methodology for obtaining a transient boundary condition that produces a prescribed interfacial surface motion to ensure a desired morphology. A systematic procedure based on the adjoint method for inverse design of solidification of binary alloys was presented by Yang and Zabaras (1998). Hale and co-workers proposed a solution technique for design and control of the temperature gradients in the unidirectional solidification problems [Hale, Keyhani, and Frankel (2000)]. Nowak et al. presented an algorithm for phase change front identification in continuous casting process [Nowak, Nowak, and Wrobel (2003)]. They formulated the problem as an inverse geometry problem, and utilized temperature measurements in the solid phase and sensitivity coefficients in the solution procedure. Okamoto and Li (2007) presented a design algorithm for optimal computation of boundary heat flux in solidification processing systems. In their method, the Tikhonov regularization method, along with the L-curve method is used to select an optimal regularization parameter. An optimal control approach for solidification process of a melt in a container was presented by Hinze and Ziegenbalg (2007). They controlled the evolution of the solid-liquid interface by the temperature on the container wall. Recently, Nowak et al. proposed a three-dimensional numerical solution of the inverse boundary problem for a continuous casting process of an aluminum alloy [Nowak, Smolka, and Nowak (2010)]. Abbasnejad et al. presented a method for optimal control of the location of both the solidus and liquidus lines in solidification of alloys [Abbasnejad, Maghrebi, Bassirat Tabrizi, Heng, Mhamdi, and Marquardt (2010)]. In their method they presented only design of simple one-dimensional solidification processes.

Almost all of the works presented in the literature on the subject of inverse solidification have been performed by the FEM and the BEM. However, being independent of a predefined mesh of elements and also suitable for the analysis of nonlinear problems, the mesh-free methods are interesting for the direct as well as inverse analysis of solidification problems. Although the BEM and FEM are well-established numerical tools for the analysis of engineering problems, the former is not quite appropriate for the analysis of nonlinear phenomena and the latter is not appropriate for the analysis of moving boundary problems. To overcome the shortcomings of the conventional numerical tools, meshless methods were introduced in the previous decade. Since the early proposal of the meshless methods, so many

researchers have contributed to the development of them and investigation on the meshless methods is still an active research area [Avila, Han, and Atluri (2011); Mirzaei and Dehghan (2011); Yang, Tang, Atluri (2011)].

In this paper, a previously developed mesh-free technique [Khosravifard and Hematiyan (2010b); Khosravifard, Hematiyan, and Marin (2011)] and the pseudo heat source method are utilized for the design of 2D solidification problems.

As mentioned earlier, the inverse analysis of solidification problems are mostly performed by the fixed and moving grid techniques. The utilization of the pseudo heat source for modeling the liberation of latent heat in inverse design of solidification problems has been reported in [Hematiyan and Karami (2003)]. Hematiyan and Karami (2003) have made use of the BEM in their analysis. Nevertheless, since the BEM is not considered as a robust technique for the analysis of nonlinear problems, the applicability of their method is limited to the linear cases, i.e. the cases for which the thermo-physical properties of the material are temperature independent. In the present paper, the concept of pseudo heat source along with a powerful truly meshless technique [Khosravifard and Hematiyan (2010b); Khosravifard, Hematiyan, and Marin (2011)] is used for the inverse design of 2D solidification problems. By using the pseudo heat source method, the inverse solidification problem transforms into a new inverse transient heat conduction problem that can be solved much more efficiently. The flux and the velocity of the liquid-solid interface are treated as secondary variables and the liquid and solid domains are modeled simultaneously. Some examples are also provided to demonstrate the effectiveness of the presented method.

2 The inverse solidification problem based on the concept of a pseudo heat source

The latent heat effects of a solidifying medium can be taken into account by considering a pseudo heat source near the moving solid-liquid interface. By considering the concept of the pseudo heat source and based on an improved meshless radial point interpolation method, a methodology is presented for the computation of an optimal distribution of heat flux history on the boundary, which results in a desired motion of the solid-liquid interface. In the present method, the fluxes on the moving boundary and its velocity are regarded as secondary variables, while the primary unknown in the inverse problem is the flux on the fixed boundaries of the problem.

The modeling of the problem can be regarded as that of fixed domain, since both the solid and liquid phases are modeled simultaneously. As a result, the equilibrium and compatibility constraints are automatically satisfied at the moving boundary. To account for the latent heat effects a moving pseudo heat source is considered

near the solid-liquid interface. The position of the heat source is updated at each time step of the problem analysis, but the interface position is fixed during each time step. In order to obtain stable and smooth results, primary and secondary regularizations are performed.

2.1 Problem statement

A liquid, which is initially at a temperature equal or above its melting temperature and occupies a domain Ω is considered. Fig. 1 depicts the problem geometry and the terminology used in this paper. A part of the fixed boundary on which prescribed boundary conditions are applied is denoted by Γ_p, and the rest of the boundary with the unknown boundary heat flux is referred to as Γ_q. The moving boundary, i.e. the solid-liquid interface, at any instant of time is denoted by $\Gamma_I(t)$. The moving boundary initially coincides with the fixed boundary $\Gamma = \Gamma_p + \Gamma_q$. Starting at the time $t = 0$ the boundary portion Γ_q is cooled and the interface proceeds inwards, generating a two-phase medium. A part of the domain that is solidified up to time t is denoted by Ω_s and the part of the domain which is still liquid is denoted by Ω_l. In the numerical formulation of the inverse problem, $n+1$ discrete time steps are considered. The objective of the problem is to find the distribution of the heat flux on Γ_q at the mentioned time steps. The part of the domain which solidifies during the time step from t_{M-1} to t_M is referred to as the transition zone and denoted by Ω_T.

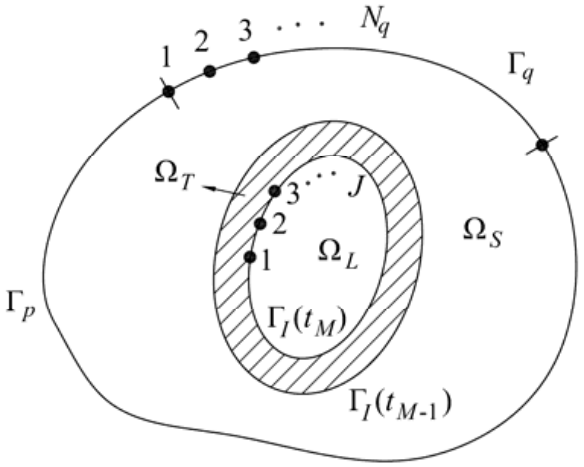

Figure 1: Geometry and terminology of the inverse solidification problem

2.2 Solution procedure

For obtaining the distribution of the heat flux on Γ_q at each time step, we adopt the function estimation approach, i.e. N_q discrete points on the boundary Γ_q are selected and a value of heat flux at each point of the boundary is obtained by the inverse analysis. In the formulation presented in this paper, Γ_I at the $n+1$ discrete time steps (t_0, t_1, …, t_n) is prescribed, and the boundary heat flux $q_B(t_i)$, $i = 1, 2, \cdots, n$ is to be so determined as to achieve the desired solid-liquid interface motion.

Suppose that the inverse problem is analyzed up to the time t_{M-1} and the heat flux $q_B(t)$ and the temperature distribution within the domain Ω is obtained at the preceding time steps $t = t_1, t_2, \cdots, t_{M-1}$. Now it is required to obtain the heat flux vector $\mathbf{q}_B$ on Γ_q for the new time step $t = t_M$. The vector $\mathbf{q}_B$ contains the values of the heat flux at the N_q points on the boundary Γ_q, i.e.

$$\mathbf{q}_B = \begin{bmatrix} q_1 & q_2 & \cdots & q_{N_q} \end{bmatrix}^{\mathrm{T}}, \tag{1}$$

In the analysis of the problem from $t = t_{M-1}$ to $t = t_M$ a pseudo heat source is applied in the transition region to model the latent heat effects. At each time step of the inverse analysis, the value of the heat source which is considered to be uniformly distributed over Ω_T is selected such that it can provide as much energy as required for the solidification of the amount of material which is enclosed in Ω_T. In this way, the intensity of the pseudo heat source can be expressed as

$$g = \frac{\rho L}{\Delta t}, \tag{2}$$

where ρ is the density of the material, L is the latent heat, and $\Delta t = t_M - t_{M-1}$.

To obtain the vector of heat fluxes $\mathbf{q}_B$, a least squares function corresponding to the inverse heat conduction problem is formed as follows [Beck, Blackwell, and St. Clair (1985)]:

$$S = (\mathbf{Y} - \mathbf{T})^{\mathrm{T}} (\mathbf{Y} - \mathbf{T}) + \alpha \mathbf{q}_B^T \mathbf{q}_B, \tag{3}$$

where the vectors $\mathbf{Y}$ and $\mathbf{T}$ contain, respectively, the values of the desired and estimated temperature at the J points on the moving interface $\Gamma_I(t_M)$. These vectors are written as

$$\mathbf{Y} = \begin{Bmatrix} Y_1 \\ Y_2 \\ \vdots \\ Y_J \end{Bmatrix}; \quad \mathbf{T} = \begin{Bmatrix} T_1 \\ T_2 \\ \vdots \\ T_J \end{Bmatrix}, \tag{4}$$

In Eq. (3), α is a regularization parameter. It should be noted that small values of α lead to oscillatory heat fluxes. Increasing the value of α decreases the oscillations; however, the difference between the desired and estimated values of the temperature increases. Consequently, proper selection of this parameter is a crucial task. In this work, the value of α is so chosen that the norm of the vector difference of the two vectors $\mathbf{Y}$ and $\mathbf{T}$ in Eq. (4) not be more than a specific value, say α_c. In problems in which the desired motion of the solidification front is physically possible, i.e. the motion is consistent with the governing physical equations, a smaller value of α_c can be chosen in comparison with the problems in which the desired motion of the solidification front violates the governing equations.

The temperature field can be represented by a Taylor's series expansion in terms of an arbitrary vector of heat fluxes $\tilde{\mathbf{q}}_B$ as follows:

$$\mathbf{T} = \tilde{\mathbf{T}} + \mathbf{X}\left(\mathbf{q}_B - \tilde{\mathbf{q}}_B\right). \tag{5}$$

The vector $\tilde{\mathbf{T}}$ is a temperature vector, obtained by an analysis of a direct problem with the vector of heat fluxes $\tilde{\mathbf{q}}_B$ applied at the boundary Γ_q. The matrix $\mathbf{X}$ in Eq. (5) is the sensitivity matrix of the problem with respect to the heat flux components, and is expressed as

$$\mathbf{X} = \begin{bmatrix} X_{11} & X_{12} & \cdots & X_{1N_q} \\ X_{21} & X_{22} & & \\ \vdots & & \ddots & \\ X_{J1} & & & X_{JN_q} \end{bmatrix}, \tag{6}$$

where

$$X_{ij} = \frac{\partial T_i}{\partial q_j}. \tag{7}$$

The simplest method for the computation of the elements of the sensitivity matrix is to use the finite difference approximation for evaluation of the derivatives.

After substituting the vector $\mathbf{T}$ from Eq. (5) into Eq. (3) and minimizing the least squares function S with respect to heat flux components, the vector $\mathbf{q}_B$ is obtained as follows [Hematiyan and Karami (2003)]:

$$\mathbf{q}_B = \left[\mathbf{X}^{\mathrm{T}}\mathbf{X} + \alpha\mathbf{I}\right]^{-1}\left[\mathbf{X}^{\mathrm{T}}\left(\mathbf{Y} - \tilde{\mathbf{T}}\right) + \mathbf{X}^{\mathrm{T}}\mathbf{X}\tilde{\mathbf{q}}\right]. \tag{8}$$

2.3 Secondary regularization

As α is increased, the oscillations in the obtained values of heat flux is reduced but the errors in the results would also be increased. After a proper selection of α, one

can utilize a so-called secondary regularization procedure to smooth the solutions [Hematiyan and Karami (2003)]. In this method, to obtain a vector $\mathbf{V}'$ with smooth elements from a vector $\mathbf{V}$ with oscillatory elements, the following relation should be minimized:

$$R = \sum_{i=1}^{M} \left(V_i' - V_i\right)^2 + \gamma \sum_{i=2}^{M-1} \left(V_{i+1}' - 2V_i' + V_{i-1}'\right)^2, \tag{9}$$

where V_i' and V_i are the elements of the vectors $\mathbf{V}'$ and $\mathbf{V}$ respectively, and M is the number of elements in each vector. γ in Eq. (9) is a regularization parameter, with the usual values between 0.5 and 5. The first term in the expression of R guarantees a vector $\mathbf{V}'$ with elements as close as possible to the elements of the vector $\mathbf{V}$. The second term reduces the oscillation of vector $\mathbf{V}'$ to produce a nearly piecewise linear distribution. The minimization of R in Eq. (9) is equivalent to minimization of the expression $\|\mathbf{S}\mathbf{V}' - \mathbf{K}\|$, where:

$$\mathbf{S} = \begin{bmatrix} \mathbf{I} \\ \gamma\mathbf{H} \end{bmatrix}; \quad \mathbf{K} = \begin{Bmatrix} \mathbf{V} \\ \mathbf{0} \end{Bmatrix}, \tag{10}$$

in which

$$\mathbf{H} = \begin{bmatrix} 0 & 0 & 0 & 0 & 0 \\ 1 & -2 & 1 & 0 & 0 \\ 0 & 1 & -2 & 1 & 0 \\ 0 & 0 & 1 & -2 & 1 \\ 0 & 0 & 0 & 0 & 0 \end{bmatrix}. \tag{11}$$

In general $\mathbf{H}$ is an $M \times M$ matrix, where M is equal to the number of elements of $\mathbf{V}$. However, Eq. (11) gives $\mathbf{H}$ for the special case with M=5.

Using a least squares approach, the vector $\mathbf{V}'$ is obtained as follows:

$$\mathbf{V}' = \left(\mathbf{S}^{\mathrm{T}}\mathbf{S}\right)^{-1}\mathbf{S}^{\mathrm{T}}\mathbf{K}, \tag{12}$$

One major characteristic of this secondary regularization scheme is that the summation of the elements of the vectors $\mathbf{V}$ and $\mathbf{V}'$ are equal. For instance, if the vector $\mathbf{V}$ describes the distribution of heat flux intensity with respect to time, then the resulted vector $\mathbf{V}'$ imposes the same amount of total energy to the domain as the vector $\mathbf{V}$ does. This point will be shown in what follows. As stated earlier, to obtain the vector $\mathbf{V}'$, the expression for R should be minimized, i.e.

$$\frac{\partial R}{\partial V_j'} = 0, \quad j = 1, 2, ..., M, \tag{13}$$

and therefore,

$$\sum_{j=1}^{M} \frac{\partial R}{\partial V_j'} = 0, \tag{14}$$

The summation of derivatives of R with respect to the elements of $\mathbf{V}'$ can be written as:

$$\begin{aligned}\sum_{j=1}^{M} \frac{\partial R}{\partial V_j'} = \sum_{j=1}^{M} \frac{\partial}{\partial V_j'} \left[\left(V_j' - V_j \right)^2 \right] + \gamma \sum_{j=2}^{M-1} \Bigg\{ & \frac{\partial}{\partial V_{j+1}'} \left[\left(V_{j+1}' - 2V_j' + V_{j-1}' \right)^2 \right] \\ & + \frac{\partial}{\partial V_j'} \left[\left(V_{j+1}' - 2V_j' + V_{j-1}' \right)^2 \right] + \frac{\partial}{\partial V_{j-1}'} \left[\left(V_{j+1}' - 2V_j' + V_{j-1}' \right)^2 \right] \Bigg\}\end{aligned} \tag{15}$$

Now, substitution of Eq. (15) into Eq. (14) results in

$$\begin{aligned}2 \sum_{j=1}^{M} \left(V_j' - V_j \right) + 2\gamma \sum_{j=2}^{M-1} \Big[& \left(V_{j+1}' - 2V_j' + V_{j-1}' \right) - 2 \left(V_{j+1}' - 2V_j' + V_{j-1}' \right) + \\ & \left(V_{j+1}' - 2V_j' + V_{j-1}' \right) \Big] = 0\end{aligned} \tag{16}$$

The second summation on the left hand side of Eq. (16) vanishes, and it can be concluded that

$$\sum_{j=1}^{M} \left(V_j' - V_j \right) = 0, \tag{17}$$

or in other words

$$\sum_{j=1}^{M} V_j' = \sum_{j=1}^{M} V_j. \tag{18}$$

which is an statement of equality of summation of elements of the two vectors $\mathbf{V}$ and $\mathbf{V}'$.

3 The meshless improved radial point interpolation method (IRPIM) formulation for the general transient heat conduction problem including heat sources

3.1 Formulation of the radial point interpolation method (RPIM)

In the RPIM, radial as well as polynomial basis functions are used for construction of shape functions. The method can be used to obtain an approximate smooth

temperature field $T^h(\mathbf{x},t)$ based on some scattered values of a temperature field $T(\mathbf{x},t)$. The approximation has the following general form:

$$T^h(\mathbf{x},t) = \sum_{i=1}^{n} \phi_i(\mathbf{x}) T_i(t) = \mathbf{\Phi}^{\mathbf{T}}(\mathbf{x})\mathbf{T}(t), \tag{19}$$

where n is the number of nodes in a supporting domain around a point of interest $\mathbf{x}$, ϕ_i is the value of the RPIM shape function corresponding to the ith node in the support domain, and $T_i(t) = T(\mathbf{x}_i,t)$ is the value of the temperature at node i, at time t. For more details on the selection of radial basis functions, and construction of the shape functions, one can refer to [Liu and Gu (2005)].

3.2 IRPIM formulation of nonlinear transient heat conduction

The general transient heat conduction equation for an isotropic medium is given as follows:

$$\nabla \cdot (k(\mathbf{x},T)\nabla T(\mathbf{x},t)) + g(\mathbf{x},T,t) = \rho(\mathbf{x},T)c(\mathbf{x},T)\frac{\partial T(\mathbf{x},t)}{\partial t}, \tag{20}$$

where ρ is the density, c is the specific heat, k is the thermal conductivity, and g is the heat generation per unit volume. The initial and boundary conditions for Eq. (20) are

$T(\mathbf{x},0) = T_0(\mathbf{x})$ in the domain (Ω),

$T = \bar{T}$ on the boundaries with the essential condition (Γ_1),

$-k(\nabla T \cdot \mathbf{n}) = \bar{q}$ on the boundaries with the natural condition (Γ_2),

where $\mathbf{n}$ is the unit outward normal vector to the boundary, T_0 is the initial condition, $\bar{T}$ is the applied temperature on the boundary, and $\bar{q}$ is the applied normal heat flux over the boundary.

On using the interpolation functions of the RPIM in the Galerkin weak form of Eq. (20), one obtains the following system of equations:

$$\mathbf{M}(T)\dot{\mathbf{T}} + \mathbf{K}(T)\mathbf{T} = \mathbf{F}(T,t), \tag{21}$$

where:

$$M_{ij} = \int_\Omega \rho(\mathbf{x},T)c(\mathbf{x},T)\phi_i\phi_j \, d\Omega, \tag{22}$$

$$K_{ij} = \int_\Omega k(\mathbf{x},T)\left[\frac{\partial \phi_i}{\partial x}\frac{\partial \phi_j}{\partial x} + \frac{\partial \phi_i}{\partial y}\frac{\partial \phi_j}{\partial y} + \frac{\partial \phi_i}{\partial z}\frac{\partial \phi_j}{\partial z}\right] d\Omega, \tag{23}$$

$$F_i = \int_{\Omega} g(\mathbf{x},T,t)\phi_i \, d\Omega - \int_{\Gamma_2} \bar{q}\phi_i \, d\Gamma. \tag{24}$$

In Eqs (22) to (24), ϕ_i and ϕ_j are the RPIM shape functions corresponding to the nodes i and j, respectively. In the conventional meshless RPIM, the domain integrals in Eqs. (22) to (24) are evaluated through a background cell structure and the Gaussian quadrature method. Consequently, the method is not truly meshless. In addition, accurate computation of domain integrals by the mentioned method in complicated domains is a time consuming task [Khosravifard and Hematiyan (2010a)]. In this paper, the above-mentioned domain integrals are evaluated with a meshless integration technique, namely the Cartesian transformation method (CTM) [Hematiyan (2007); Hematiyan (2008)].

3.3 The CTM for evaluation of domain integrals in the meshless IRPIM

For the numerical analysis of both the nonlinear heat conduction and the solidification problems by the mesh-free methods, a large number of domain integrals should be evaluated. Such domain integrals should be evaluated in every iteration of each time step of the numerical analysis. As a result, the fast and accurate evaluation of such domain integrals is a crucial task in the overall performance of the mesh-free methods [Khosravifard, Hematiyan and Marin (2011)]. In addition, if the formulation of the mesh-free method used for the analysis of the problem is based on the global weak-form, the domain integrals should be evaluated over the entire problem domain. Consequently, utilization of a meshless integration technique for computation of domain integrals of the mesh-free methods can be very attractive. In this paper, the CTM is used for evaluation of domain integrals in the formulation of the inverse problem. In this way, the overall efficiency of the method is improved. Bui et al. have found the CTM highly appropriate for the evaluation of domain integrals in mesh-free methods [Bui, Nguyen, and Zhang (2011)].

According to the CTM procedures, a domain integral can be evaluated by the dot product of two vectors containing the values of the CTM integration weights and the values of the integrand at the CTM integration points [Khosravifard and Hematiyan (2010a)]:

$$I = \int_{\Omega} f(\mathbf{x}) \, d\Omega \approx \sum_{i=1}^{N} W_i^{CTM} \times f(\mathbf{x}_i) = \mathbf{W}^{CTM} \cdot \mathbf{F}, \tag{25}$$

where, N is the total number of CTM integration points in the domain, W_i^{CTM} is the CTM integration weight associated with the ith integration point, located at $\mathbf{x}_i$. Detailed explanations on the methods for computation of the CTM integration weights and points can be found in [Khosravifard and Hematiyan (2010a)].

As an example, the evaluation of the mass matrix in Eq. (22) by the CTM is as follows:

$$M_{ij} = \sum_{l=1}^{N} W_l^{2D} \left(R_l \times C_l \times S_{i,l} \times S_{j,l} \right), \tag{26}$$

where, R_l and C_l are the values of the density and specific heat of the material at the lth CTM integration point repectively, and $S_{i,l}$ is the value of RPIM shape function at the lth CTM integration point. Similar expressions for Eqs. (23) and (24) can be found in [Khosravifard and Hematiyan (2010b); Khosravifard, Hematiyan, and Marin (2011)].

4 Numerical examples

To study the effectiveness of the proposed method, three example problems are analyzed. In the first example, a physically feasible motion of the solid-liquid interface is considered, and the corresponding history of heat flux on the fixed boundary is obtained. In the second and third examples, freezing front motions which violate the governing equations, and therefore are not physically possible, are selected. In each case, a heat flux history that results in an interface motion that best matches the desired freezing front motion is obtained.

4.1 Example 1: A unidirectional solidification problem, with varying interface velocity

In this example, solidification of a casting in a long and narrow mold with a varying front velocity is simulated and designed. The problem geometry and boundary conditions are shown in Fig. 2 (a). Fig. 2(b) depicts the nodal distribution used in the meshless IRPIM. The design objective of this example is to achieve a unidirectional motion of the freezing front, parallel to the line AB, by computation of an optimal value for the heat flux on the boundary line AB. It is required that the velocity of the solidification front vary uniformly from 10^{-4} m/s at the beginning of the process to 5×10^{-4} m/s when the whole casting is solidified. It is also required that the whole solidification process takes place in 300 seconds. The material properties of the casting are k =240 W/m˚C, c=950 J/kg˚C, ρ=2700 kg/m^3, and L=397 kJ/kg. Both the melting and initial temperatures of the casting are 660 ˚C.

The inverse problem is analyzed once by considering 5 time steps ($\Delta t = 60$ s) and once by 10 time steps ($\Delta t = 30$ s), and the results are compared. 15 sampling points are selected on the moving boundary, and 6 points are selected on the boundary line AB for the sake of computation of the required heat flux. It should be stated that as

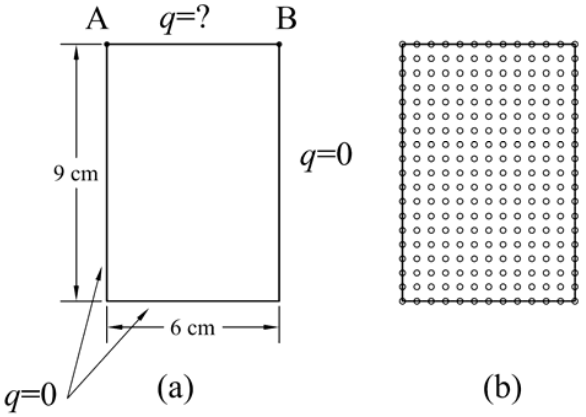

Figure 2: Configuration of example 1: (a) the geometry and boundary conditions; (b) the nodal arrangement of the meshless IRPIM

the moving front gets further away from the fixed boundary line AB, the control of the front motion by application of heat flux on the boundary becomes more difficult.

The numerical solutions are performed with the meshless IRPIM [Khosravifard and Hematiyan (2010b); Khosravifard, Hematiyan, and Marin (2011)]. The obtained values for the average heat flux output from the boundary line AB is given in Tab. 1. The results presented in this table are obtained without performing the secondary regularization. From the results given in this table for the case with 10 time steps, it can be inferred that some temporal oscillations in the results are present. In this table, by t_{end} we mean the time at the end of each time step.

Table 1: The average value of heat flux (KW/m^2) on the boundary line AB, example 1.

t_{end}	30	60	90	120	150	180	210	240	270	300
5 steps	159	159	214	214	354	354	503	503	677	677
10 steps	145	178	182	250	355	364	529	504	717	711

Fig. 3, depicts the location of the freezing front at various instances of time, as obtained by applying the computed values of the heat flux at the boundary line AB. To obtain the designed front position, a direct enthalpy-based solidification analysis is performed by ANSYS with a fine mesh.

In order to damp the temporal oscillations in the results, a secondary regularization is performed. To visualize the effect of this regularization in reduction of oscilla-

tions in the computed heat flux, the results obtained with and without regularization are depicted in Fig. 4.

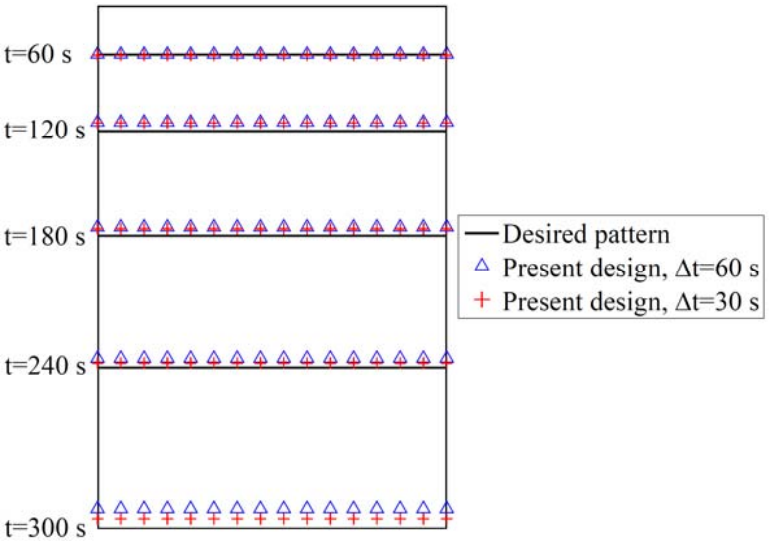

Figure 3: The solid-liquid interface position obtained by the present method, example 1

By performing a direct solidification analysis based on the computed values of the heat flux, the position of the solidification front at discrete instances of time is computed. These locations that correspond to the fluxes reported in Fig. 4 are presented in Tab. 2. In this table, y_1 and y_2 denote the positions of the solidification front computed by a direct analysis based on the heat fluxes obtained with and without secondary regularization. It can be seen that utilization of the secondary regularization, even improves the ability of the inverse analysis in computation of heat fluxes that results in the desired motion of the solidification front.

As stated earlier, the computational labor of the inverse analysis based on the con-

Table 2: The position of the solidification front, obtained from fluxes with and without secondary regularization

t (s)	60	120	180	240	300
Desired position (cm)	8.16	6.84	5.04	2.76	0
y_1 (with secondary regularization)	8.19	6.93	5.10	2.80	0.18
y_2 (without secondary regularization)	8.15	6.98	5.16	2.84	0.17

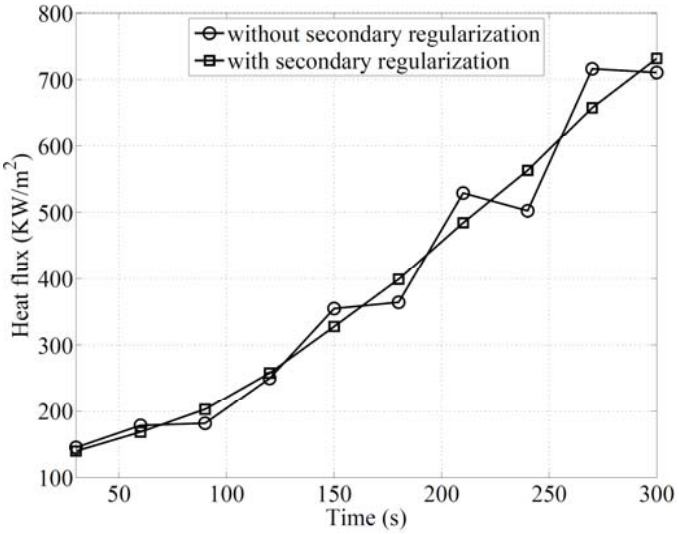

Figure 4: Reduction of oscillations in the results by the use of secondary regularization in example 1

cept of pseudo heat source is much less than the inverse analysis based on the conventional fixed or moving grid techniques. The total computational time for this example, for the case with $\Delta t = 60$ s is 97 seconds. While the direct analysis of this example by the meshless IRPIM with the same nodal distribution in a time interval of 60 seconds, would take about 400 seconds. Considering the point that in an inverse analysis several direct problems should be solved for the sensitivity analysis, the amount of time saved by using the pseudo heat source method is significant. The computational times reported here are based on developed codes in MATLAB and run on a PC system with an Intel (R) Core™2 Quad CPU Q9550 @ 2.83 GHz and 4.00 GB of RAM.

4.2 Example 2: Design of a continuous casting process

In this example, a continuous casting process is designed. The problem geometry and boundary conditions are shown in Fig. 5. In this figure, the desired motion of the solid-liquid interface is shown by the dashed lines. The solid-liquid interface moves inwards parallel to the fixed boundaries at a constant speed of 5×10^{-4} m/s. It should be noted that the desired solidification front motion is physically impossible because of the steep corners. The aim of this example is to find a heat flux history that results in an interface motion that best matches the desired freezing front motion.

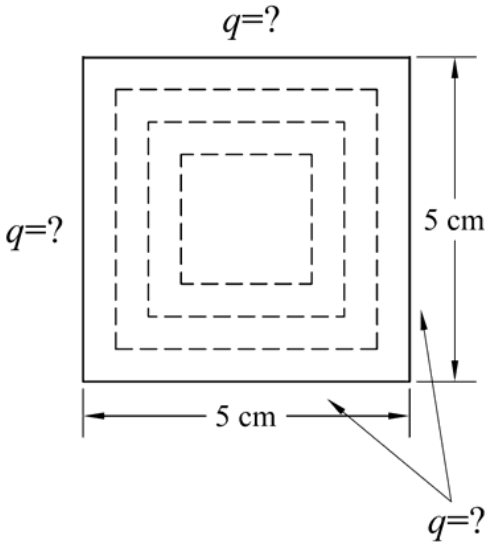

Figure 5: The problem specification of example 2

The material properties of the casting are$k$ =34 W/m˚C, c=475 J/kg˚C, ρ=7800 kg/m^3, and L=271 kJ/kg. Both the melting and initial temperatures of the casting are 1450 ˚C.

In this example, one can make use of the existing symmetry of the problem, and only one eighth of the geometry can be modeled. The geometrical model of the numerical method, along with the nodal distribution of the meshless IRPIM is shown in Fig. 6.

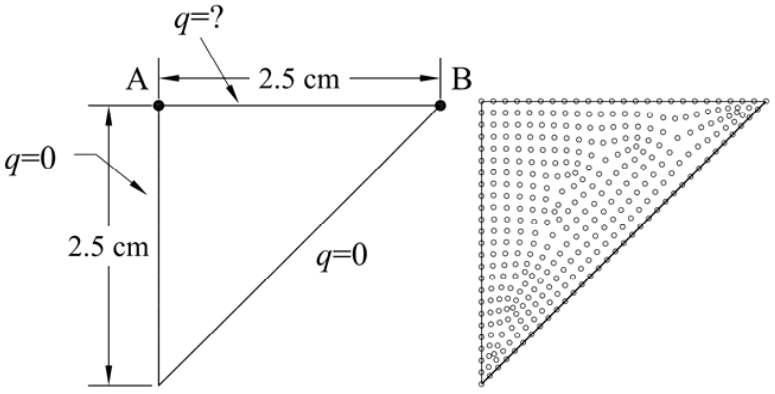

Figure 6: The geometrical model and nodal distribution of the numerical method

For the inverse analysis of this example, 5 time steps are used, and the values of the heat fluxes are computed at the beginning of each time step. Also, six points on the boundary line AB (Fig. 6) are chosen, at which the values of heat flux are computed. Fig. 7, depicts the computed values of the heat flux on the boundary line AB at various instances of time.

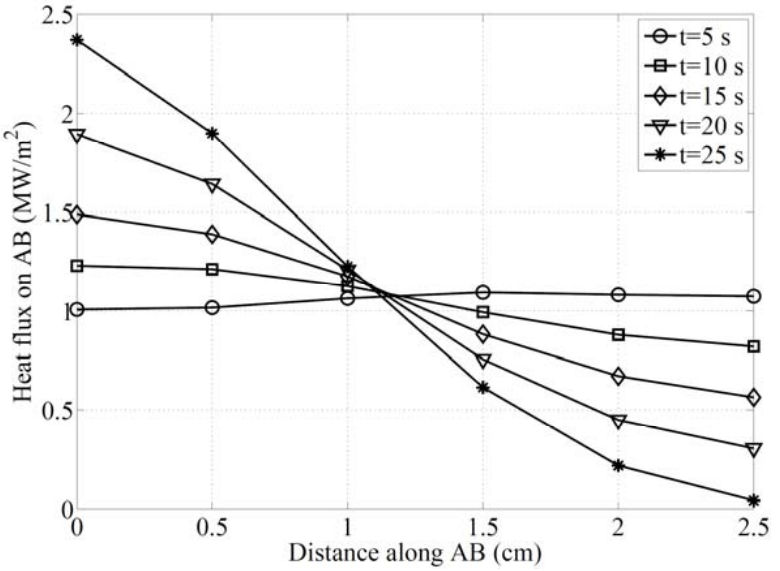

Figure 7: Heat flux on the boundary line AB at various instances of time, example 2

Fig. 8 depicts the location of the freezing front at various instances of time, as obtained by applying the computed values of the heat flux at the boundary line AB. To obtain the estimated front position, a direct enthalpy-based solidification analysis is performed by ANSYS.

4.3 Example 3: Inverse Design of a directional solidification problem

In this example, a directional casting process is designed. The problem geometry and boundary conditions are shown in Fig. 9. In this figure, the desired motion of the solid-liquid interface is shown by the dashed lines. The dashed lines represent the desired position of the solidification front in intervals of 20 seconds. In this example, the solidification front makes an angle with the boundary line AB, and this angle increases with time.

In this example, the desired solidification front which is also contour of $T = T_m$ is

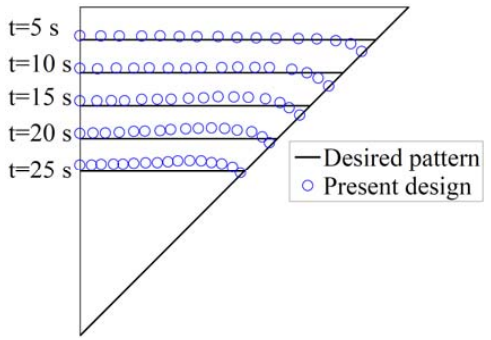

Figure 8: The solid-liquid interface position obtained by the present method, example 2

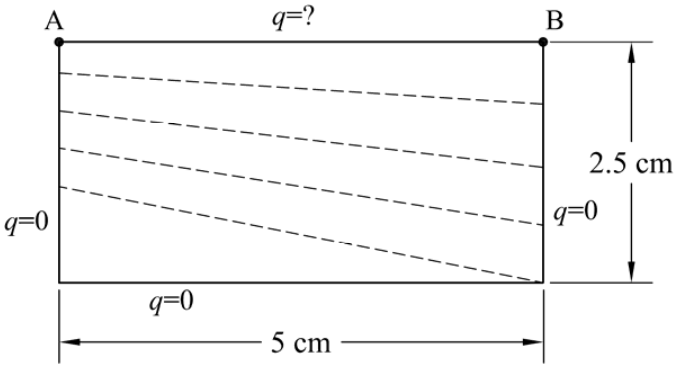

Figure 9: The geometry and boundary conditions of example 3

not perpendicular to the insulated boundaries. Consequently, the desired motion of the solidification front is not physically possible. By the inverse analysis of this example, a distribution of heat flux history on boundary line AB that would result in a front motion that best matches the desired motion will be obtained.

The material properties of the casting are$k$ =35 W/m˚C, c=450 J/kg˚C, ρ=7800 kg/m^3, and L=271 kJ/kg. Both the melting and initial temperatures of the casting are 1406 ˚C.

To investigate the effect of the number of nodes of the meshless method on the accuracy of the results, three nodal distributions are selected and the problem is solved with each distribution. These nodal distributions of the meshless IRPIM are shown in Fig. 10.

Using the nodal distributions shown in Fig. 10, the optimum value of heat flux

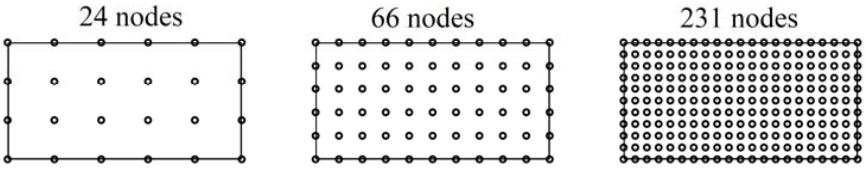

Figure 10: Nodal distributions of the meshless IRPIM, example 3

on the boundary line AB for each case is obtained. Based on the obtained values of the heat flux and a direct analysis performed by ANSYS with a fine mesh, the position of the solidification front for each case is obtained. The position of the solidification front for each case in comparison with the desired position is plotted in Fig. 11. This figure shows that as the number of nodes in the numerical method increases, the estimated position of the solidification front gets closer to the desired one. However, even for the case with a small number of nodes, the results are acceptable. This means that in the present method, with a small computational labor, a fairly acceptable distribution of heat flux can be obtained.

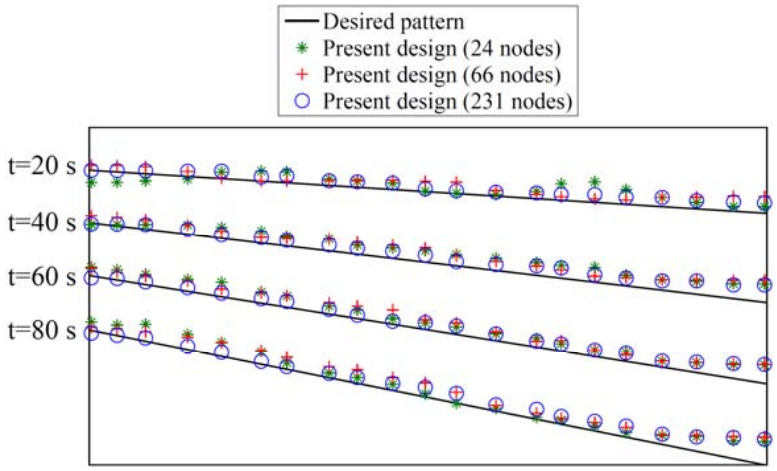

Figure 11: The solid-liquid interface position obtained by the present method, example 3

Although all the three nodal distributions of the meshless method yield acceptable results for the position of the solidification front, as the number of nodes increases, the oscillations of the heat flux decrease. Figs. 12, 13, and 14 depicts the variation of heat flux on the boundary line AB for the cases with 24, 66, and 231 nodes,

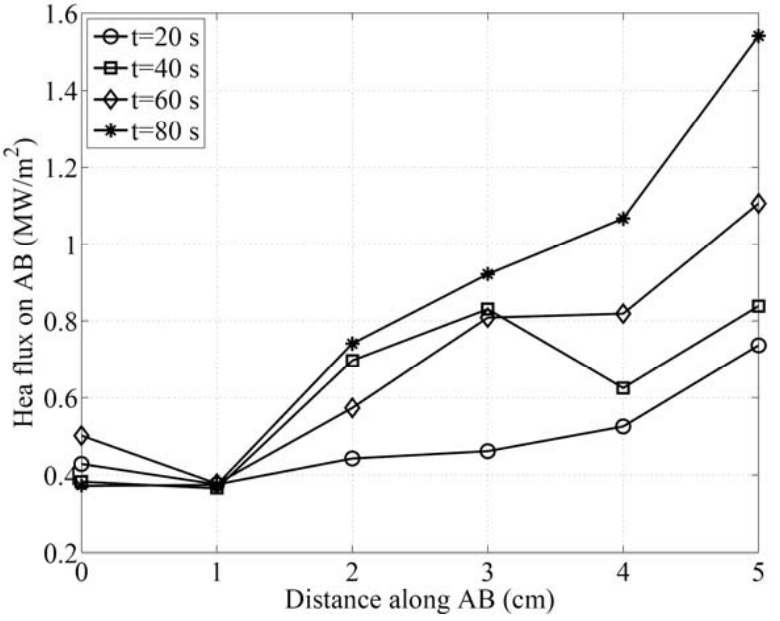

Figure 12: Heat flux on the boundary line AB, obtained by 24 node

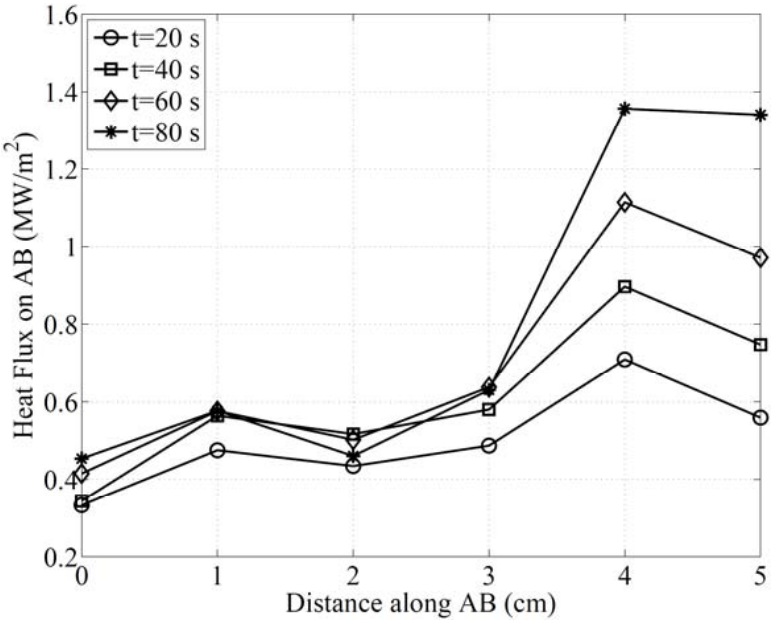

Figure 13: Heat flux on the boundary line AB, obtained by 66 nodes

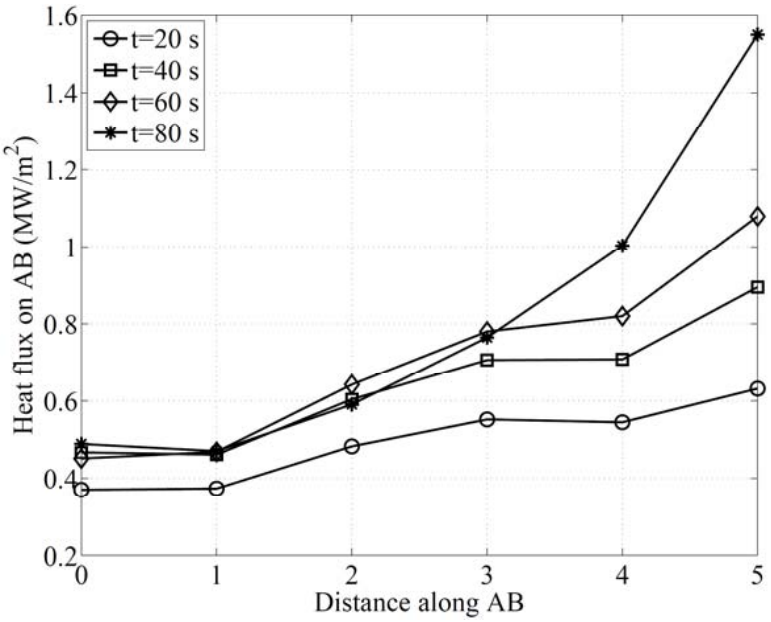

Figure 14: Heat flux on the boundary line AB, obtained by 231 nodes

respectively.

5 Conclusion

Based on the concept of pseudo heat source method and the use of an improved meshless RPIM, a procedure for optimal calculation of heat fluxes in solidification processes was presented. The presented method, converts an inverse solidification problem into a much simpler inverse heat conduction problem. As a result, the computational cost of the presented procedure is much lower than other inverse solidification methods. Sequential and secondary regularizations are performed to damp the oscillations. Three examples were presented that demonstrate the usefulness of the presented technique. By the numerical examples, it was concluded that increasing the number of nodes in the meshless method, results in smoother heat fluxes.

References

Abbasnejad, A.; Maghrebi, M.J.; Bassirat Tabrizi, H.; Heng, Y.; Mhamdi, A.; Marquardt, W. (2010): Optimal operation of alloy material in solidification processes with inverse heat transfer. *International Communications in Heat and*

Mass Transfer, vol. 37, pp. 711–716.

Avila, R.; Han, Z.; Atluri, S.N. (2011): A novel MLPG-Finite-Volume Mixed Method for Analyzing Stokesian Flows & Study of a new Vortex Mixing Flow. *CMES: Computer Modeling in Engineering & Sciences*, vol. 71, no. 4, pp. 363–396.

Beck, J.V.; Blackwell, B.; St. Clair, C.R. (1985): *Inverse Heat Conduction: Ill posed Problems*. Wiley Interscience.

Bui, T.Q.; Nguyen, M.N.; Zhang, Ch. (2011): An efficient meshfree method for vibration analysis of laminated composite plates. *Computational Mechanics*, vol. 48, no. 2, pp. 175–193.

Frankel, J.I.; Keyhani, M. (1996): A new approach for solving inverse solidification design problems. *Numerical Heat Transfer, Part B*, vol. 30, pp. 161–177.

Hale, S.W.; Keyhani, M.; Frankel, J.I. (2000) Design and Control of interfacial temperature gradients in solidification. *International Journal of Heat and Mass Transfer*, vol. 43, pp. 3795–3810.

Hematiyan, M.R. (2007): A general method for evaluation of 2D and 3D domain integrals without domain discretization and its application in BEM. *Computational Mechanics*, vol. 39, pp. 509–520.

Hematiyan, M.R. (2008): Exact transformation of a wide variety of domain integrals into boundary integrals in boundary element method. *Communications in Numerical Methods in Engineering*, vol. 24, no. 11, pp. 1497–1521.

Hematiyan, M.R.; Karami, G. (2003): A boundary elements pseudo heat source method formulation for inverse analysis of solidification problems. *Computational Mechanics*, vol. 31, pp. 262–271.

Hinze, M.; Ziegenbalg, S. (2007): Optimal control of the free boundary in a two-phase Stefan problem. *Journal of Computational Physics*, vol. 223, pp. 657–684.

Kang, S.; Zabaras, N. (1995): Control of the freezing interface motion in two-dimensional solidification processes using the adjoint method. *International Journal for Numerical Methods in Engineering*, vol. 38, pp. 63–80.

Katz, M.A.; Rubinsky, B. (1984): An inverse finite-element technique to determine the change of phase interface location in one-dimensional melting problems. *Numerical Heat Transfer*, vol. 7, pp. 269–283.

Khosravifard, A.; Hematiyan, M.R. (2010a): A new method for meshless integration in 2D and 3D meshfree Galerkin method. *Engineering Analysis with Boundary Elements*, vol. 34, pp. 30–40.

Khosravifard, A.; Hematiyan, M.R. (2010b): Nonlinear transient thermo-mechanical analysis of functionally graded materials by an improved meshless radial point in-

terpolation method, *Advances in Boundary Element techniques XI, BETEQ 2010, 12-14 July, Berlin*.

Khosravifard, A.; Hematiyan M.R.;Marin, L. (2011): Nonlinear transient heat conduction analysis of functionally graded materials in the presence of heat sources using an improved meshless radial point interpolation method. *Applied Mathematical Modelling*, vol. 35, pp. 4157–4174.

Liu, G.R.; Gu, Y.T. (2005): *An Introduction to Meshfree Methods and their Programing*, Springer.

Mirzaei, D.; Dehghan, M. (2011): MLPG Method for Transient Heat Conduction Problem with MLS as Trial Approximation in Both Time and Space Domains. *CMES: Computer Modeling in Engineering & Sciences*, vol. 72, no. 3, pp. 185–210.

Nowak, I.; Nowak, A.J.; Wrobel, L.C. (2003): Inverse analysis of continuous casting processes. *International Journal of Numerical Methods for Heat and Fluid Flow*, vol. 13, pp. 547–564.

Nowak, I.; Smolka, J.; Nowak, A.J. (2010): An effective 3-D inverse procedure to retrieve cooling conditions in an aluminum alloy continuous casting problem. *Applied Thermal Engineering*, vol. 30, pp. 1140–1151.

Okamoto, K.; Li, B.Q. (2007): A regularization method for the inverse design of solidification processes with natural convection. *International Journal of Heat and Mass Transfer*, vol. 50, pp. 4409–4423.

Ruan, Y.; Zabaras, N. (1991): An inverse finite element technique to determine the change of phase interface location in two-dimensional melting problems. *Communications in Applied Numerical Methods*, vol. 7, pp. 325–338.

Voller, V.R. (1992): Enthalpy method for inverse Stefan problems. *Numerical Heat Transfer, Part B*, vol. 21, pp. 41–55.

Yang, C.; Tang, D.; Atluri, S. (2011): Patient-Specific Carotid Plaque Progression Simulation Using 3D Meshless Generalized Finite Difference Models with Fluid-Structure Interactions Based on Serial *In Vivo* MRI Data. *CMES: Computer Modeling in Engineering & Sciences*, vol. 72, no. 1, pp. 53–78.

Yang, G.Z.; Zabaras, N. (1998): The adjoint method for an inverse design problem in the directional solidification of binary alloys. *Journal of Computational Physics*, vol. 140, pp. 432–452.

Zabaras, N. (1990): Inverse finite element techniques for the analysis of solidification processes. *International Journal for Numerical Methods in Engineering*, vol. 29 (1990), 1569–1587.

Zabaras, N.; Mukherjee, S.; Richmond. O. (1988): An analysis of inverse heat

transfer problems with phase changes using an integral method. *Journal of Heat Transfer*, vol. 110, pp. 554–561.

Zabaras, N.; Nguyen, T.H. (1995): Control of the freezing interface morphology in solidification processes in the presence of natural convection. *International Journal for Numerical Methods in Engineering*, vol. 38, pp. 1555–1578.

Zabaras, N.; Ruan, Y.; Richmond, O. (1992): Design of two-dimensional Stefan processes with desired freezing front motions. *Numerical Heat Transfer, Part B*, vol. 21, pp. 307–325.

Zabaras, N.; Yuan, K. (1994): Dynamic programming approach to the inverse Stefan design problems. *Numerical Heat Transfer, Part B*, vol. 26, pp. 97–104.